GastroPlus is a mechanistically based simulation software package that simulates intravenous, oral, oral cavity, ocular, inhalation, dermal/subcutaneous, and **NEW!** intramuscular absorption, pharmacokinetics, and pharmacodynamics in humans and animals. This smoothly integrated platform combines a user-friendly interface with powerful science to help you make faster and more informed project decisions!

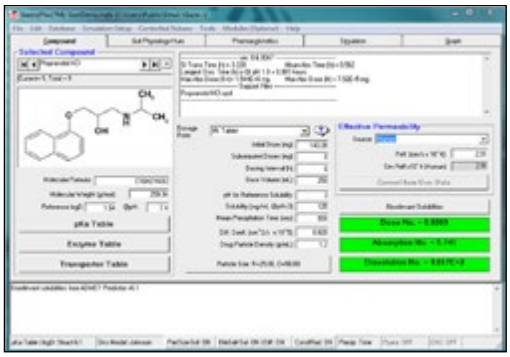

GastroPlus is by far the most commonly used software of its kind. It has been identified as the #1-ranked program for *in vitro - in vivo* extrapolation (IVIVE) and has been the focus of several publications from the FDA!

The GastroPlus simulations include:

FOR DISSOLUTION & ABSORPTION -

- The Advanced Compartmental Absorption and Transit (ACAT™) model – only in GastroPlus!
- Physiological gut models for human, dog, rat, mouse, rhesus monkey, cynomolgus monkey, minipig, rabbit and cat – fasted or fed conditions defined
- Vast selection of dosage forms: immediate release, delayed release, controlled release (including dispersed systems, gastric-retention, and more)
- pH-dependent solubility and logD models – ionization effects on dissolution & absorption considered
- Paracellular absorption – estimate paracellular permeability
- Mechanistic effect of bile salts on drug solubility and dissolution
- Enhanced treatment of nanoparticle effects on solubility and dissolution
- Mechanistic models to predict *in vivo* precipitation
- Options for defining pH-dependent dissolution (Z-factor) and precipitation rates
- Saturable metabolism and/or influx/efflux transport along the GI tract
- Mechanistic deconvolutions and *in vitro - in vivo* correlations (IVIVCs) for various formulations

FOR PHARMACOKINETICS -

- Whole body, physiologically-based pharmacokinetic (PBPK) models defined – including **pediatrics**
- One-, two-, or three-compartment conventional pharmacokinetic model options available
- Transporter-based IVIVE: automated scaling of permeability across all tissues with PBPK
- Saturable metabolism and transport in liver or any PBPK tissues
- Metabolite tracking – easily link the formation of metabolites with the metabolism of the parent(s) in a single simulation
- Mechanistic treatment of biliary secretion and enterohepatic circulation
- Mechanistic static and dynamic DDI predictions
- Automated PBPK/PD model selection with industry standard pharmacodynamic models

Simulation Modes Available -

- Population Simulator™ – predict likely distributions of PBPK/PD results over different populations
- Parameter Sensitivity Analysis – quickly test sensitivity of results to changes in model parameters
- Batch Simulations – screen compound libraries for bioavailability & PK exposure in different species

SimulationsPlus SCIENCE + SOFTWARE = SUCCESS Please call for more information +1-661-723-5523 | sales@simulations-plus.com

Coming Soon in Version 9.6!

- **ACAT™ model**: **NEW!** dynamic intestinal fluid model
- **PBPKPlus™ Module**: **Improved!** covariates when generating populations, **Additional!** disease physiologies (obesity, renal impairment), **NEW!** clearance mechanisms in blood compartments
- **Metabolism and Transporter Module**: **Expanded!** enzyme/transporter distribution information
- **DDI Module**: **Additional!** compound model files for substrates & inhibitors
- **IVIVCPlus™ Module**: **NEW!** time scale/shift correlation & triple Weibull functions
- **PDPlus™ Module**: **NEW!** bacteria killing PD models
- **Improved!** output/reporting functions and simulation performance (speed)
- … and more!

Available Now in Version 9.5!

- **NEW!** PBPK models for antibody-drug conjugates (ADCs)
- **NEW!** PBPK physiology models for Chinese (pediatric and adults) and hepatic impairment populations
- **NEW!** Bolus & controlled release models for subcutaneous and intramuscular injections
- **Updated!** Animal physiology models for non-oral delivery pathways
- **Improved!** Reporting functions – easy export into Excel spreadsheets
- **Upgraded!** Automated mechanistic deconvolutions and easier virtual BE simulation setup
- **Enhanced!** More covariate relationships in the Population Simulator
- … and more!

ADMET Predictor™ Module

CYP metabolism predictions from chemical structure – quickly create full PBPK models in seconds.

The ADMET Predictor™ Module extends the capability of GastroPlus by enabling you to obtain predictions from structure of all physico-chemical, pharmacokinetic, and CYP metabolism kinetic parameters required for GastroPlus PBPK simulations. The module uses the same models as our best-in-class ADMET Predictor software.

Updated! Enhanced pKa model developed in collaboration with **Bayer HealthCare** - ALL models retrained with greater accuracy!

This module automatically generates predictions for the following properties:

- CYP metabolism kinetics – Vmax, Km, and CLint
- P-gp and OATP transporter inhibition models (classification)
- Aqueous solubility vs. pH profile
- Biorelevant solubility (FaSSIF, FeSSIF, and FaSSGF)
- logD vs. pH profile
- Rabbit corneal permeability
- Human volume of distribution
- Blood:brain barrier permeation (classification)
- pKa(s)
  - Tendency to supersaturate in water
  - Diffusion coefficient in water
  - Human effective permeability
  - Human plasma protein binding
  - Human blood:plasma concentration ratio

The ADMET Predictor Module has several critical benefits:

(1) by loading a library of chemical structures, you can quickly set up a database for screening fraction absorbed & bioavailability – decide which compounds to carry forward into *in vivo* studies
(2) use the *in silico* predictions and Parameter Sensitivity Analysis to guide your *in vitro* studies
(3) begin evaluating different formulation strategies to assess the importance of factors like particle size, solubility and dose on absorption

PBPKPlus™ Module

Ranked #1 in *in vitro-in vivo* Extrapolation (IVIVE) by Pfizer!
(Cole et al., 2nd Asian Pacific Regional ISSX Meeting, May 2008, Shanghai, China)

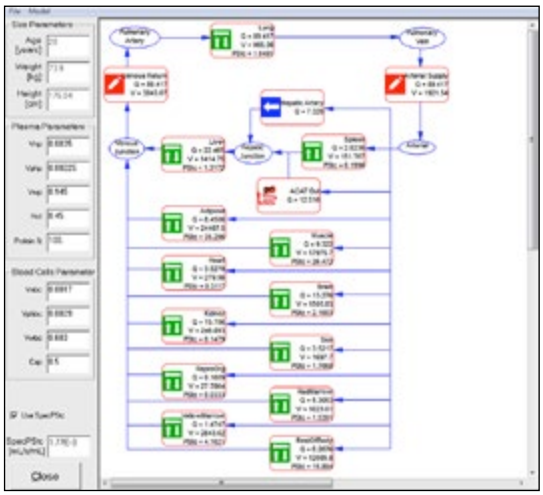

Only in GastroPlus! Transporter-based IVIVE: automated scaling of permeability across tissues in the PBPK model

The PBPKPlus Module extends GastroPlus to define a "whole body" PK model, consisting of various tissues. You can easily simulate the distribution & elimination of compound throughout the body and track concentrations in any tissue. Tissues can be defined as needed, or default models can be used with a standard set of compartments:

Adipose	Arterial blood	Brain	Yellow marrow
Gut	Heart	Lungs	Kidney
Liver	Muscle	Skin	Red marrow
Spleen	Reproductive organs	Venous blood	

Customize your PBPK model by treating any tissue as either a perfusion-limited or permeability-limited model, and quickly add/delete tissues as needed – all without writing any equations!

The PBPKPlus Module also provides:

- Generation of physiological model parameters (tissue weights and volumes, composition, perfusion rates, etc...) with our built-in PEAR Physiology™ (Population Estimates for Age-Related Physiology).

Current physiologies are:

- Human (American, Japanese, and **NEW!** Chinese, Male or Female, based on age)
- Infant/pediatric groups
- **NEW!** Hepatic impairment
- **NEW!** Renal impairment
- **NEW!** Obesity
- Rat
- Dog
- Mouse
- Monkey
- Rabbit
- Minipig

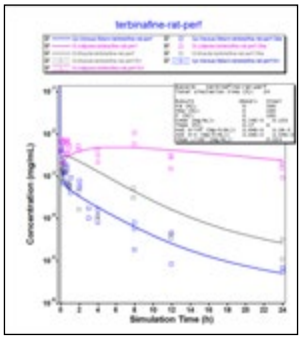

- Population simulations based on parameter variances in a sample population – define your own age range, % male vs. female, and the number of "virtual" subjects you wish to create
- Novel methods for estimating tissue partition coefficients from logD, pKa, plasma protein binding and Rbp – only in GastroPlus!
- Physiological model for kidney including glomerular filtration and reabsorption
- Fitting models to *in vivo* data (plasma/tissue concentrations, amount excreted in urine, etc...)
- Linking of pharmacodynamic effect directly to concentrations in specific tissues
- Mechanistic transport of drug from hepatocytes to bile in liver, modeled either as a linear process or through carrier-mediated transport
- Report-quality plotted output of all time-dependent results in all tissues
- ... and more!

SimulationsPlus SCIENCE + SOFTWARE = SUCCESS
Please call for more information +1-661-723-5523 | sales@simulations-plus.com

Drug-Drug Interaction (DDI) Module

The DDI Module in GastroPlus allows you to predict drug-drug interactions (DDIs) among drugs and metabolites.

The ability to accurately estimate potential DDIs *in silico* has several benefits for companies:

- Explore possible effects on the pharmacology and toxicology of drugs
- Identify species-specific changes to estimate how a drug behaves in animals vs. humans
- Investigate the safety profile of drugs that are co-administered prior to filing regulatory submissions with agencies around the world

With the DDI Module, calculating either steady-state and/or dynamic DDIs is managed through our easy-to-use interface. We provide a database of standard compounds for which all relevant parameters (including reported inhibition/induction constants and full compartmental PK/PBPK models) are defined. Of course, you may predict DDIs among any compounds by simply entering the required inputs. As with other GastroPlus modules, there is no equation or code writing required.

What are some of the advantages to using the DDI Module?

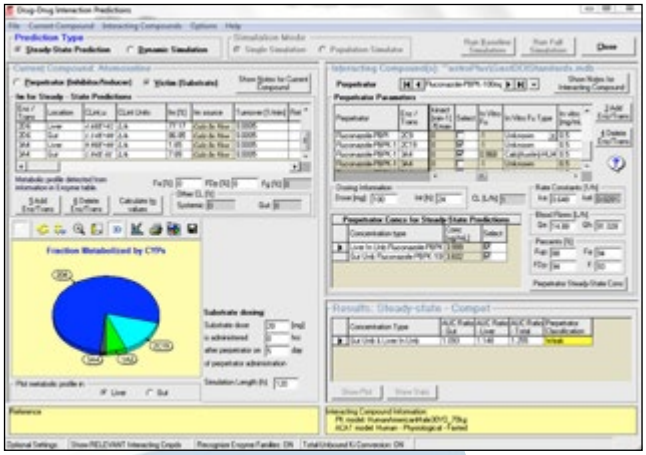

- **NEW!** PBPK models for DDI standard compounds
- Population Simulator™ linked with DDI predictions
- Transporter-based drug-drug interactions
- Metabolic and/or transporter induction
- Linked with the industry's #1-ranked dissolution/absorption (ACAT™) model
- Use with either compartmental PK or PBPK models
- Apply competitive and/or time-dependent inhibition kinetics by parent and/or metabolite(s)
- Simulate DDIs for any species
- Account for enzyme expression level differences in various human populations
- Built-in tool to easily calculate the fraction metabolized (fm) from *in vitro* assays (rCYPs and microsomes are accommodated)
- Incorporate nonlinear gut contributions to DDIs
- Predict the inhibitor effect using simulated concentrations at the site of metabolism (gut, liver, or any PBPK tissue) for dynamic DDI simulations
- Include the effects of multiple substrates on clearance of other substrates metabolized by the same enzyme

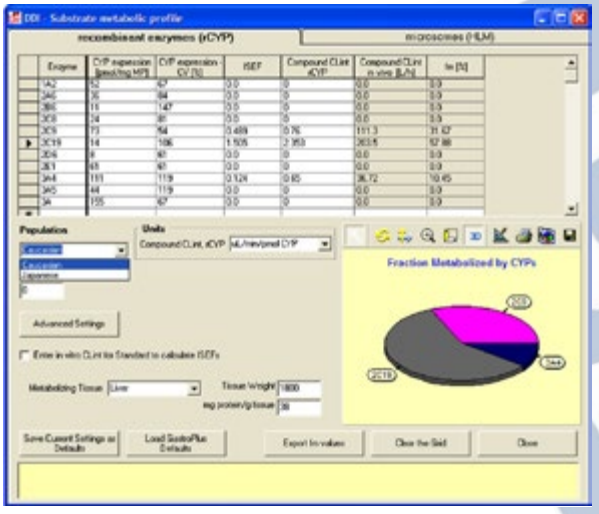

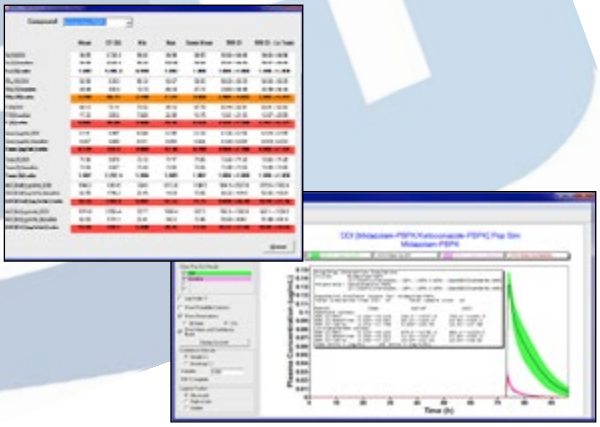

Additional Dosage Routes Module

The Additional Dosage Routes Module in GastroPlus extends the program beyond the traditional oral and intravenous administration routes. With this module, you can simulate drug disposition through additional dosing sites – dermal, intraoral (oral cavity), ocular, pulmonary (intranasal and respiratory), and **NEW!** intramuscular. These models were all developed in collaboration with top 5 pharmaceutical companies. The ability to predict concentration profiles in different regions of the skin, mouth, eye, lungs, nose, and muscle can help you:

- Explore various formulation/drug delivery options to achieve desired therapeutic effects
- Identify species-specific changes to estimate how a drug is handled in animals vs. humans

With the Additional Dosage Routes Module, simulating concentrations through these sites is managed through our easy-to-use interface. Mechanistic, physiologically-based models are provided for each tissue, for different species. You can also customize your own physiology by entering available information into the program. These models are linked with either compartmental or physiologically-based pharmacokinetics (PBPK) in GastroPlus, so you may predict your drug's distribution and elimination once it enters into the systemic circulation. As with other GastroPlus modules, there is no equation or code writing required.

Ocular Model (Ocular Compartmental Absorption & Transit (OCAT™) Model

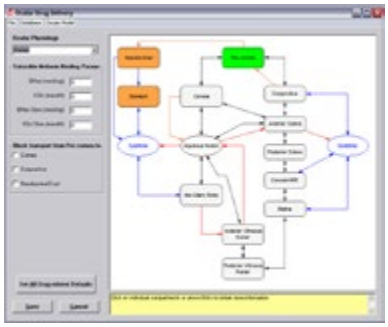

- Nonlinear metabolism or transport in any eye tissue!
- Two-site melanin binding options!
- Convective flow incorporated into the ocular disposition model
- Physiology models (human, rabbit, and **NEW!** monkey)

The ocular model of the Additional Dosage Routes Module provides dosing as:

- Eye drop (topical solution or suspension)
- Intravitreal or subconjunctival implants
- IVT (intravitreal injection)

Some of the processes which can be modeled include:

- Nonlinear metabolism or transport in any eye tissue
- Convective flow incorporated into the ocular disposition model
- Two-site melanin binding options
- Predefined physiology models (human, rabbit, and **NEW!** monkey)

Pulmonary (Intranasal/Respiratory) Model (Pulmonary Compartmental Absorption & Transit (PCAT™) Model

- Nonlinear metabolism or transport in any lung tissue!
- Age-dependent scaling of the pulmonary physiology!
- Physiology models (human, rat, **NEW!** mouse, and **NEW!** dog)

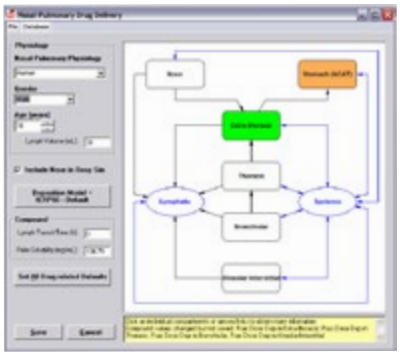

The pulmonary model provides dosing via the intranasal or respiratory route as an:

- Immediate release solution
- Immediate release powder

The pulmonary model includes the advanced ICRP 66 deposition model (Smith et al., 1999, LUDEP) for calculating deposition fractions in each compartment of both API and carrier particles. Additionally, you may account for the following processes in your simulations:

- Mucociliary transit
- Nonlinear metabolism or transport in any lung tissue
- Lymphatic transport & systemic absorption
- Age-dependent scaling of the human physiology

Dermal/Subcutaneous Model

The Transdermal Compartmental Absorption & Transit (TCAT™) model represents the skin as a collection of the following compartments: stratum corneum, viable epidermis, dermis, subcutaneous tissue, sebum, hair lipid, and hair core. The subcutaneous tissue is also considered. The diagram is shown in the figure below.

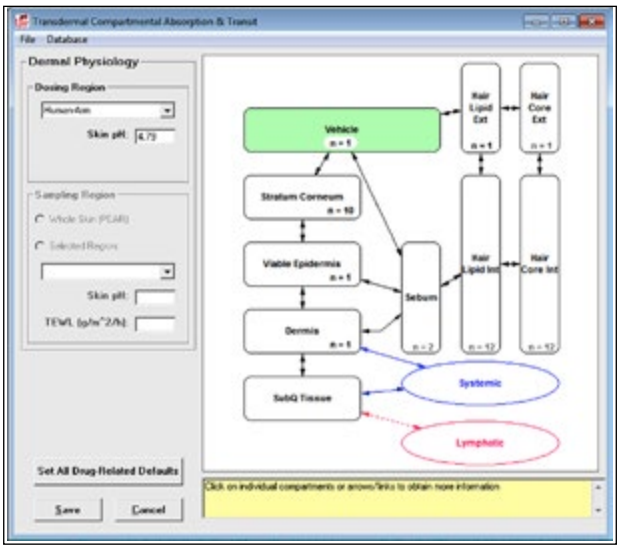

The model can simulate a variety of transdermal & subcutaneous dosage forms, specified at different places on the body, including:

- liquid formulations (solutions, lotions, suspensions)
- semi-solid formations (gels, creams, lotions, pastes)
- subcutaneous injections (bolus or controlled release)

Some of the processes modeled include:

- vehicle evaporation
- absorption from the vehicle into the various tissue regions
- nonlinear metabolism in any tissue region
- systemic circulation and lymphatic absorption

Measured *in vivo* data for any dermal tissue can be used to compare with simulation results. All standard GastroPlus features, including the Population Simulator and Parameter Sensitivity Analysis, can be used with the dermal model.

Oral Cavity Delivery Model

The Oral Cavity Compartmental Absorption & Transit (OCCAT™) model represents the oral cavity (mouth) as a collection of the following compartments: buccal, gingival, palate, top of the tongue, bottom of the tongue, and mouth floor. The diagram is shown in the figure at right.

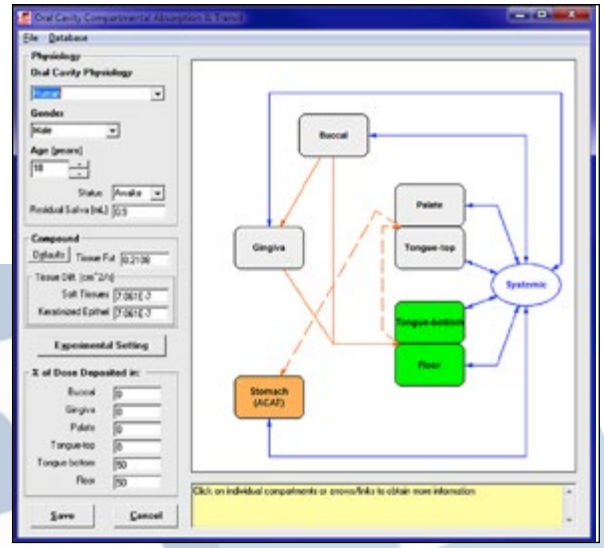

The model can simulate a variety of dosage forms including:

- sublingual solutions & tablets
- lingual sprays & supralingual tablets
- controlled release buccal patches

Some of the processes modeled include:

- dissolution & precipitation in the saliva
- diffusion through the oral mucosa
- uptake into systemic circulation
- swallowing of unabsorbed drug

Measured *in vivo* data for any oral cavity tissue can be used to compare with simulation results. All standard GastroPlus features, including the Population Simulator and Parameter Sensitivity Analysis, can be used with the oral cavity model.

Metabolism and Transporter Module

When linked with the upgraded ADMET Predictor™ Module, predict CYP metabolism pathways & kinetics, and have the Enzyme Table automatically populated with the correct locations and units!

Updated! Enzyme and transporter expression levels across species – including UGTs and SULTs!

Enhanced! Metabolite tracking options!

The Metabolism and Transporter Module is an optional module that extends the capabilities of GastroPlus to include saturable metabolism and carrier-mediated transport into any compartment (gut, liver, and/or any PBPK tissue), along with metabolite tracking. This module calculates Michaelis-Menten rates for gut and liver (or any PBPK tissue) metabolism and for carrier-mediated transport (influx or efflux) based on input values for Vmax and Km. You can provide Vmax and Km values for each enzyme/transporter independently, or you can lump them into a single effective Vmax and Km, depending on your data. The distribution factors on the Physiology tab are automatically loaded for recognized gut enzymes and transporters, and provide the relative amounts of enzymes or transporters in the various ACAT™ gut model compartments. The Vmax and Km scale factors on the Pharmacokinetics tab are provided to allow fitting nonlinear kinetic models to your data.

The Metabolism and Transporter Module includes a Units Converter for easy transformation of a variety of your *in vitro* metabolism or transporter kinetic parameters into parameters and units that can be utilized by the GastroPlus model.

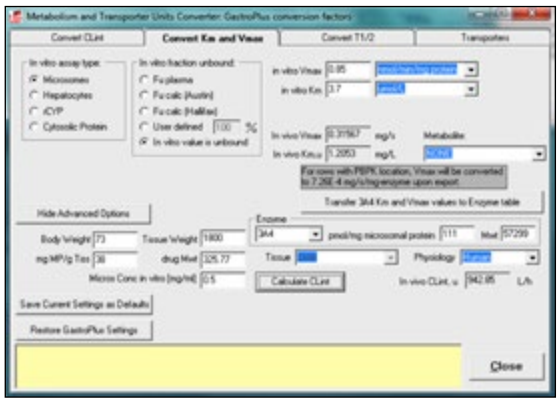

The Units Converter window that provides a convenient way of converting *in vitro* measurements to *in vivo* inputs for the GastroPlus model.

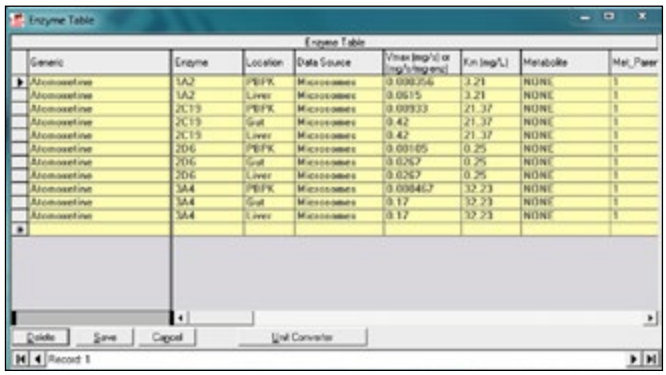

Define multiple metabolic / transport pathways, with enzymes and transporters placed into the tissues or organs of your choice! Also link formation of different metabolics in a single simulation!

New article from FDA scientists compare the Mechanistic Absorption deconvolution in GastroPlus vs. traditional methods – conclusion is that GastroPlus provides "greater predictive accuracy" - Mirza et al., Pharm. Res. 2012

IVIVCPlus is an optional add-on module that provides a convenient way to develop a correlation between either *in vitro* release and *in vivo* release or *in vitro* release and absolute bioavailability. The formed correlation can then be used to predict PK profiles for formulations with different *in vitro* release rates.

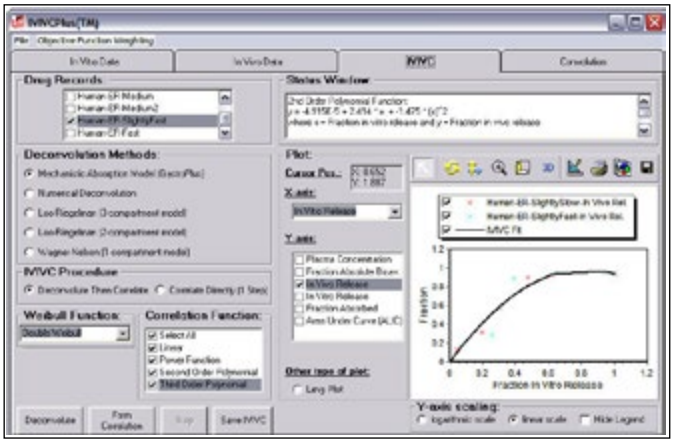

GastroPlus was the first software program to offer "mechanistic deconvolutions", which deconvolute, or fit, the *in vivo* dissolution vs. time along the gut lumen. An advantage to using the mechanistic deconvolution method is that it can be linked to a PBPK model. We are pleased to validate the mechanistic deconvolution method through a 5-year **Research Collaboration Agreement with the U.S. FDA**.

IVIVCPlus offers five methods for deconvolution:

1) Mechanistic Absorption Model (GastroPlus)
2) Numerical Deconvolution
3) Loo-Riegelman (2-compartment model)
4) Loo-Riegelman (3-compartment model)
5) Wagner-Nelson (1-compartment model)

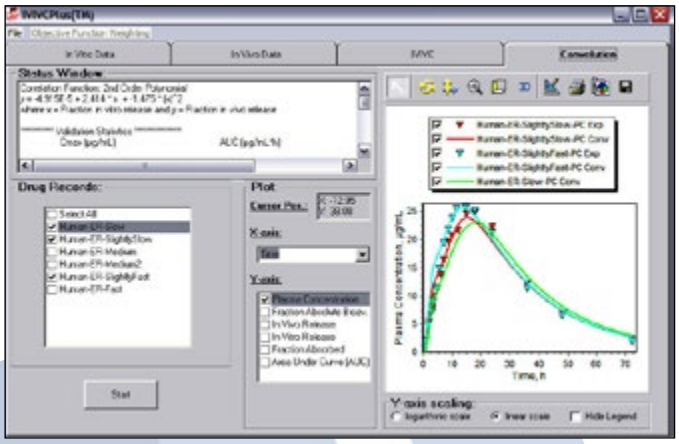

The Mechanistic Absorption Model (GastroPlus) deconvolution method directly deconvolutes the *in vivo* release rate. The other four methods are traditional deconvolution methods that calculate the rate of appearance of compound into the systemic circulation. For formulation scientists, the correlation between *in vitro* release and *in vivo* release is much more intuitive and valuable.

Depending on the deconvolution method selected, a correlation can be made between *in vitro* release and *in vivo* release or *in vitro* release and absolute bioavailability. Currently, linear, power, and polynomial (second or third order) functions may be selected for the functional form of the correlation.

Run Convolutions: The correlation function can be used to calculate an *in vivo* release-time profile or absolute bioavailability-time profile for a new formulation of the compound exhibiting a different *in vitro* release-time profile. A plasma concentration-time profile for the new formulation can be constructed with the calculated *in vivo* release-time or absolute bioavailability-time profile.

Evaluate Validation Statistics: After running a convolution, IVIVCPlus outputs the observed values, predicted values, prediction errors, and mean absolute percent prediction error for both Cmax and AUC. These statistics can be used to evaluate the internal or external predictability of the correlation as described in the FDA's "Guidance for Industry Extended Release Oral Dosage Forms: Development, Evaluation, and Application of *In Vitro*/*In Vivo* Correlations".

PKPlus™ Module

PKPlus extends GastroPlus to rapidly estimate pharmacokinetic (PK) parameters for non-compartmental analysis (NCA), along with 1-, 2-, & 3-compartment models from IV and oral plasma concentration-time (Cp-time) data, without the need to run full simulations. The fitted parameters include PK parameters, first order absorption rate, bioavailability and absorption lag time (if both IV and oral data are included in fitting). Required inputs are Cp-time profiles, dose, body weight and infusion time (if applicable). Compartmental PK can be fitted to single IV or oral data as well as across multiple Cp-time profiles - IV, oral, or combination of IV and oral as well as different dose levels. Linear or saturable clearance models can be selected easily.

Full statistics, including Akaike Information Criterion and R^2, are provided for all models. Residual information is also captured and can be plotted. Once finished in PKPlus, the parameter values of the selected model can be easily transferred back to the main GastroPlus model, and all model results can be saved into report-quality outputs.

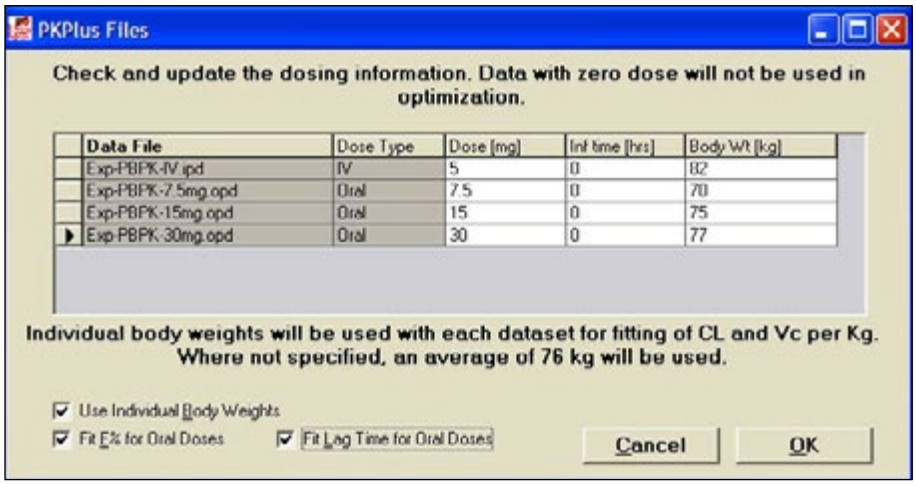

Plotting of absolute, log, and residuals for each model is selected with a mouse click, allowing rapid comparison of models.

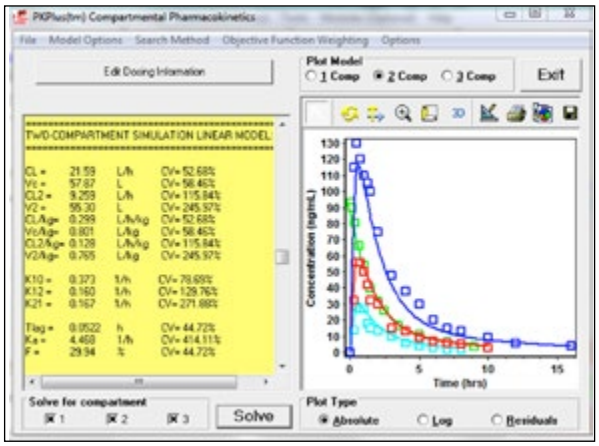

2-compartment model for midazolam fitted across IV and three oral doses

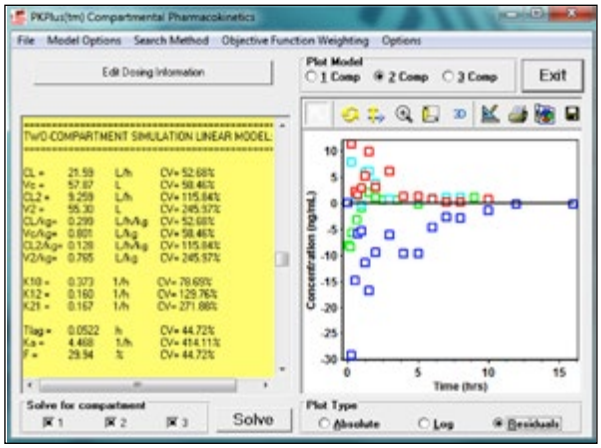

Residuals plot for 2-compartment model for midazolam fitted across IV and three oral doses

Enhanced! Automated model selection – fit across all direct and indirect models, along with phase-nonspecific cell killing options, with a single mouse click!

PDPlus allows you to fit standard pharmacodynamic (PD) models to observed data and use the fitted models to predict PD effect changes due to changes in dose, dosage form, and dosing regimens. The PDPlus module adds the Pharmacodynamics Table, which contains the PD model, the site of PD action, and the parameters that determine the kinetics of the action. Multiple PD models (therapeutic and adverse) can be accommodated for each drug record.

Updated! Easily fit PD models across multiple data sets (e.g, doses)

With PDPlus, fitting pharmacodynamic models to observed effect data is quick and easy. You may fit any of the standard PD models:

Direct Link: Linear, Log Linear, Emax and Sigmoid Emax

Indirect Link: Class 1, Class 2, Class 3, Class 4

Other: Phase-nonspecific cell killing (for tumor PBPK/PD modeling)

Convenient plotting of both plasma concentration-time and effect vs. time or concentration is provided with absolute and log plots available for each. Plus, all model results can be saved into report-quality outputs.

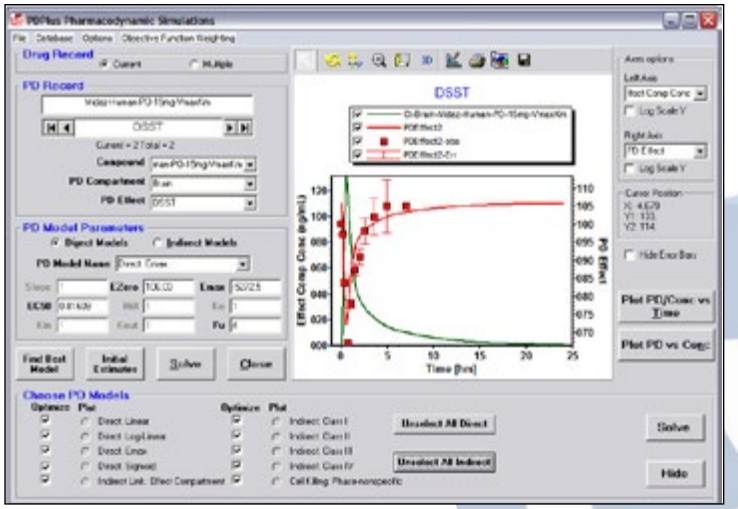

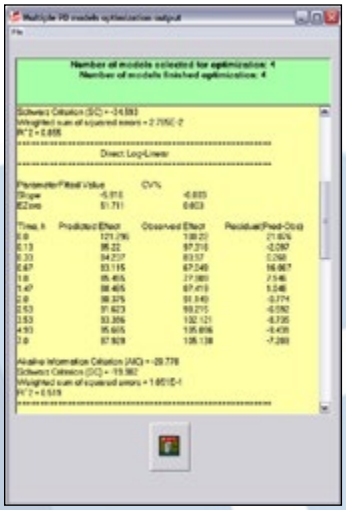

The effect can be linked directly to drug concentration in a specific tissue to easily perform PBPK/PD modeling.

The Optimization Module for GastroPlus extends and enhances the program's basic capabilities in several important ways:

- To automatically fit model parameters to data
- To optimize study designs (e.g., dosing regimens) and dose

Fitting models to data

One of the most important uses of GastroPlus is to fit absorption, pharmacokinetic, and pharmacodynamic models to observations. In doing so, researchers gain tremendous insight into how their compound is behaving *in vivo*. When a single set of model parameters can be found that properly describes the observed plasma concentration-time for all dose levels, a useful model has been obtained. In general, if the model parameters must be changed for each dose level, then something is not being accounted for correctly. The Optimization Module performs the multidimensional search needed to fit model parameters to one or more data sets automatically.

Model fitting can include (but is not limited to):

- PBPK model parameters to plasma and/or tissue concentration vs. time data
- Peff and absorption scale factors to determine regional dependencies
- A wide variety of physiological parameters (when necessary)
- Parameters to match profiles of parent drugs or any of their metabolites

Model parameters can be fitted to data for a single record, or across multiple records simultaneously. The program will run one simulation for each record each time it changes the value(s) of one or more model parameters. Typically, hundreds of iterations will be performed, each with N simulations, where N is the number of records whose observations are being used to compare predicted and observed values. Objective function weighting is user-defined, and includes the most common weighting schemes.

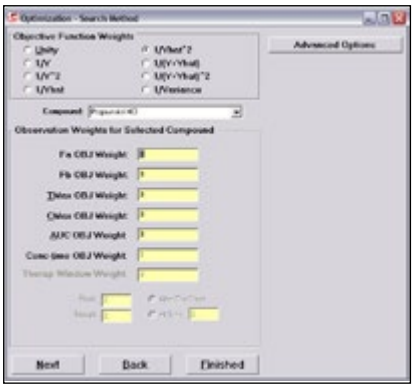

Biologics Module

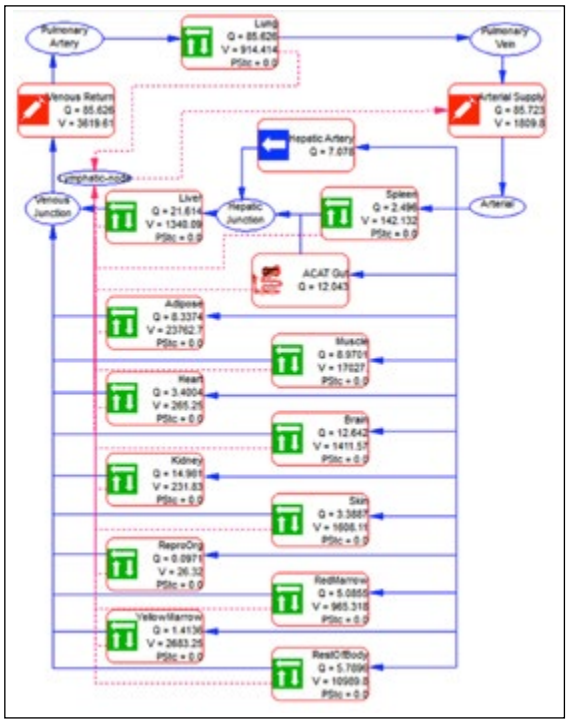

Each organ in the PBPK model is divided into three major compartments representing the vascular, endosomal, and interstitial spaces, as shown in the image at right.

NEW! PBPK models for antibody-drug conjugates (ADCs)

Starting in GastroPlus 9.0, we are pleased to offer PBPK models for large molecules (biologics). The Biologics Module simulates the absorption, distribution, and clearance of biological drugs. In the current implementation, both monoclonal antibodies (mAb) and antibody-drug conjugates (ADCs) administered as an intravenous bolus dose, intravenous infusion, or subcutaneous (SQ) injection can be modeled. As with other GastroPlus modules, there is no equation or code writing required. A schematic diagram of how the different organs are connected to one another is shown at left.

All major organs are connected in an anatomical fashion with plasma flow represented by blue solid arrows and lymph flow by red dashed arrows. The lymph node collects the lymphatic drainage from organs and lymph fluid is returned to the systemic circulation. Each organ in the PBPK model is divided into three major compartments representing the vascular, endosomal, and interstitial spaces, as shown below.

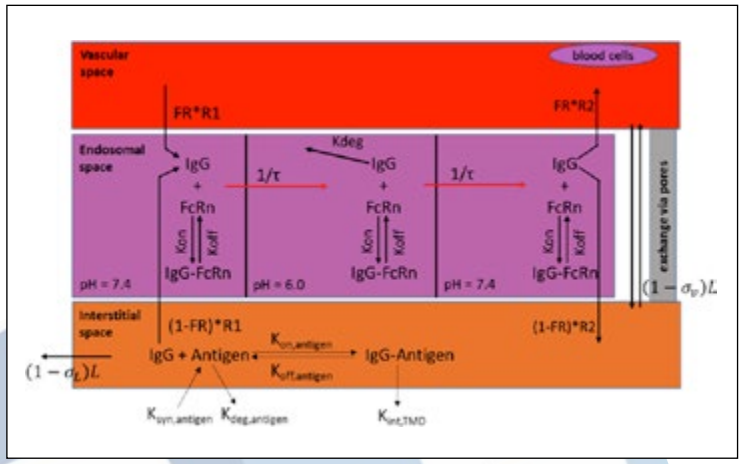

Some of the key processes accounted for in the GastroPlus models include:

- Convective transport and fluid phase endocytosis describing uptake of antibody into the tissue
- mAb-FcRn (neonatal FC receptor) binding & recycling
- Target mediated elimination in the interstitial space to include the influence of specific antigen-mAb interactions on mAb disposition
- Within the endosomal space, the competition for binding to FcRn between endogenous IgG and the therapeutic mAb
- mAb administration by either intravenous (IV) or subcutaneous (SQ) injection
- Complete default physiology parameters for humans – flexibility to create custom species models
- With ADCs, distribution and elimination processes of multiple ADC species with different DAR (drug-to-antibody ratio):
  - o Distribute to peripheral compartments
  - o Cleared by nonspecific clearance
  - o Bind to target receptor, internalize, and be cleared in the cell lysosome

W5237

Mechanistic Absorption and Physiologically Based Pharmacokinetic Modeling of Itraconazole and Its Application for Drug-Drug Interaction with Midazolam in Adult Populations

Ke X. Szeto, Viera Lukacova, John DiBella, Walter S. Woltosz, and Michael B. Bolger

Simulations Plus, Inc., 42505 10th Street West, Lancaster, CA 93534, USA

Introduction

Itraconazole (ITZ) is a BCS Class II triazole antifungal (Sporanox; Janssen Pharmaceutica, Titusville, NJ). It is a substrate and potent inhibitor of CYP3A4. The primary metabolite hydroxy-itraconazole (OH-ITZ) and the two other downstream metabolites, keto-itraconazole (keto-ITZ) and N-desalkyl-itraconazole (ND-ITZ), are also substrates and inhibitors of CYP3A4. The purpose was to develop a mechanistic absorption model (MAM)/PBPK model for ITZ and its metabolites which accounts for all the relevant mechanisms (dissolution, precipitation, absorption, distribution, metabolism, and auto-inhibition) after i.v. and p.o. ITZ administration.. This model was validated by predicting effect of ITZ administration on midazolam (MID) pharmacokinetics (PK).

METHODS

The PBPKPlus™ module in GastroPlus™ (Simulations Plus, Inc.) was used to model the PK of ITZ and the three metabolites. The Advanced Compartmental Absorption and Transit (ACAT™) model was used to describe the intestinal dissolution, precipitation, and absorption of ITZ after p.o. administration. Human physiologies were generated by the program's internal Population Estimates for Age-Related (PEAR™) Physiology™ module. Tissue/plasma partition coefficients for all the compounds were calculated using the Lukacova algorithm based on tissue composition and *in vitro* and *in silico* physicochemical properties. The biopharmaceutical parameters for both ITZ and its metabolites were either obtained from literature or predicted by ADMET Predictor™ 6.5 (Simulations Plus, Inc.). The metabolism series from ITZ to OH-ITZ to keto-ITZ to ND-ITZ (all mediated by the CYP3A4 enzyme) was modelled by Michaelis-Menten kinetics with *in vitro* enzyme kinetic parameters and the GastroPlus built-in expression levels of CYP3A4 in gut and liver. The default dissolution model was used for both solution and capsule dosage forms. Particle size for the capsule dosage form was adjusted to 3 µm to account for the formulation effect. The program's mechanistic nucleation and growth (MNG) model was used to account for possible precipitation as ITZ solubility changes in different intestinal regions. The permeability of ITZ was predicted in MembranePlus™ 1.0 (Simulations Plus, Inc). The DDI module in GastroPlus was used to predict the effect of ITZ on MID PK for a variety of study designs (varying ITZ and MID doses and administration times).

Table 1. Ki and Km values[4]

	Ki,u (nM)	Km,u (nM)
ITZ	1.3	3.9
OH-ITZ	14.4	27
Keto-ITZ	1.4*	1.4
ND-ITZ	0.38#	0.38

*Ki,u is the same as Km,u

#Km,u and Ki,u were calculated from IC50,u based on the incubated MDZ concentration 1 uM

The results of selected doses are shown below:

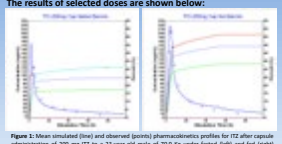

Figure 1: Mean simulated (line) and observed (points) pharmacokinetics profiles for ITZ after capsule administration of 200 mg ITZ to a 23-year-old male of 70.9 Kg under fasted (left) and fed (right) condition. Blue colored lines and data points represent plasma concentration (y-axis on the left). The remaining lines represent cumulative amount of ITZ dissolved, absorbed, entering portal vein, entering systemic circulation, and total precipitated, all shown as percent of the administered dose (y-axis on the right)

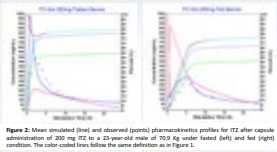

Figure 2: Mean simulated (line) and observed (points) pharmacokinetics profiles for ITZ after capsule administration of 200 mg ITZ to a 23-year-old male of 70.9 Kg under fasted (left) and fed (right) condition. The color-coded lines follow the same definition as in Figure 1.

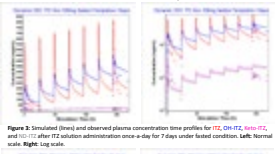

Figure 3: Simulated (lines) and observed plasma concentration time profiles for ITZ, OH-ITZ, Keto-ITZ, and ND-ITZ after ITZ solution administration once-a-day for 7 days under fasted condition. **Left:** Normal scale. **Right:** Log scale.

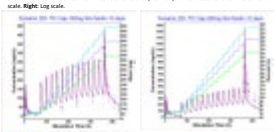

Figure 4: Simulated (purple lines) and observed plasma concentration time profiles (purple squares) for ITZ after ITZ capsule administration once-a-day for 15 days under fed condition. **Left:** 100 mg once a day. **Right:** 200 mg once a day. The remaining lines represent cumulative amount of ITZ dissolved, absorbed, entering portal vein and entering systemic circulation, all shown as percent of the administered dose (y-axis on the right).

Results

Part I: Overall performance on ITZ-MDZ drug-drug interaction prediction.

Table 2 summarizes the literature data on drug-drug interaction between ITZ and MID [5-9]. The first three studies used solution dosage forms while the rest used capsule dosage forms of ITZ. The demographic information and study protocol are also provided in the same table. On the day of MID administration, we assumed the subjects were in fed state for 3 hours after lunch and then switched to fasted state. Since both MID and ITZ are sensitive to prandial states, it is important to specify the physiological changes according to the meal schedule in the DDI simulations.

Table 2. DDI study design details

Trial No.	1	2	3	4
ITZ	50 mg SD	200 mg SD	400 mg SD	200 mg SD
Midazolam	2 mg taken 4 hours after the inhibitor dose	2 mg taken 4 hours after the inhibitor dose	2 mg taken 4 hours after the inhibitor dose	7.5 mg po taken 2 hours after the inhibitor dose on day 1
Demographics of HVs (M:F)	n=6 (5:1); age 22-42 yrs	n=6 (5:1); age 22-42 yrs	n=6 (5:1); age 22-42 yrs	n=12 (7:5); age 19-25 yrs; weight 57-95 kg
Study Protocol	Didn't mention, assumed Fasted	Didn't mention, assumed Fasted	Didn't mention, assumed Fasted	Volunteers fasted for 3 hours.
Reference	Templeton et al. 2010	Templeton et al. 2010	Templeton et al. 2010	Olkkola et al. 1996

Trial No.	5	6	7	8	9
ITZ	200 mg QD for 6 days	100 mg QD for 4 days	200 mg QD for 6 days	200 mg QD for 4 days	200 mg QD for 4 days
Midazolam	0.05 mg/kg IV over 2 min, 2 hours after the inhibitor dose on day 4	7.5 mg po taken 2 hours after the inhibitor dose on day 4	7.5 mg po taken 2 hours after the inhibitor dose on day 6	15 mg taken 2 hours after the inhibitor dose on day 4	7.5 mg po taken 1 hour after the inhibitor dose on day 4
Demographics (M:F)	n=12 (7:5); age 19-25 yrs; weight 57-95 kg	n=12 (4:8); age 19-30 yrs; weight 54-98 kg	n=12 (7:5); age 19-25 yrs; weight 57-95 kg	n=9 (4:5); age 22-34 yrs; weight 55-78 kg	n=9 (2:7); age 19-26 yrs; weight 52-85 kg
Study Protocol	Volunteers fasted for 3 hours.	Volunteers fasted for 3 hours.	Volunteers fasted for 3 hours.	Volunteers fasted for 2 hours.	Volunteers fasted for 3 hours.
Reference	Olkkola et al. 1996	Ahonen et al. 1995	Olkkola et al. 1996	Backman et al. 1998	Olkkola et al. 1994

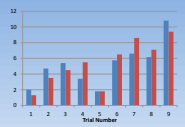

Figure 5: Predicted (blue) and observed (green) fold changes in AUC ratios for midazolam under ITZ inhibition effect. Note that study 9 has been corrected for gender effect on CYP3A4 expression level.

Part II: DDI Contribution from ITZ and its metabolites

Lastly, in this section, we discuss the individual contribution of ITZ and its metabolites to the overall DDI effect. Here we simulated the inhibition effect of 100mg ITZ on oral MID tablets (7.5 mg) 4 days after the treatment. Table 3 summarizes the predicted AUC ratios under different model settings: 4 competitive substrates (ITZ, hydroxyl-ITZ, keto-ITZ, ND-ITZ), 3 substrates (ITZ, hydroxyl-ITZ, keto-ITZ), 2 substrates (ITZ, hydroxyl-ITZ) and 1 substrate (ITZ). The metabolites contributed about 45% of the total change of AUC and ND-ITZ was the main contributor among all the metabolites. This result is consistent with data published in literature suggesting that ND-ITZ was the most potent inhibitor among ITZ and its metabolites [10], and that 50% of inhibition is associated with the metabolites of ITZ [5].

Table 3. DDI contribution from ITZ and its metabolites.

ITZ model (number of subs)	4	3	2	1	Obs Values[6]
AUC_competitive (ng-h/mL)	433.10	303.60	269.30	244.50	586
AUC_baseline (ng-h/mL)	66.10	66.10	66.10	66.10	102
Ratio of AUC's	6.55	4.59	4.07	3.70	5.75

CONCLUSIONS

The work demonstrates the use of the GastroPlus MAM/PBPK approach to predict DDI interactions involving not only perpetrator, but its multiple metabolites (and metabolites of metabolites). The MAM/PBPK approach incorporates all relevant processes in drug absorption, distribution, metabolism, and elimination and helps with prediction of PK for different dosage forms and study designs. Including all the major downstream metabolites of ITZ was important for accurate prediction of the DDI effect. The overall results presented in Figure 5 show that the model predicts accurately across different studies for both solution and capsule doses using the MNG precipitation model. To conclude, we have shown that the GastroPlus MAM/PBPK approach, integrating relevant physicochemical processes and physiological details, is a highly valuable and reliable predictive utility.

References:

[1] Stevens DA, Pharmacotherapy 1999;19(5):603–611.
[2]. Heykants J, Mycoses 32 (Suppl. 1) 67-87.
[3] Lukacova V. Poster presentation, AAPS 2008, Atlanta GA
[4] Isoherranen N, GMD 2004; 32:1121–1131
[5]. Templeton I, Clin Pharmacol Ther. 2010;88(4):499-505
[6] Ahonen J, Br J Clin Pharmacol 1995; 40:270-272.
[7]. Backman JT, Eur J Clin Pharmacol 1998; 54: 53-58.
[8]. Olkkola KT, Anesth Analg 1996; 82: 511-516.
[9]. Olkkola KT, Clin Pharmacol Ther 1994; 55(5): 481-485.
[10]. Vera JS, Pharmacotherapy 1996; 16(3):424-428

R6307

Physiologically based pharmacokinetic (PBPK) model for prediction of vancomycin pharmacokinetics in children

Lukacova, V. , W.S. Woltosz, M.B. Bolger

Simulations Plus, Inc. Lancaster, California, USA; correspondence should be addressed to: viera@simulations-plus.com

Aim

Ethical considerations prevent extensive clinical trials in pediatric populations; however, with the use of PBPK modeling, *in vivo* data from adults can be used to explore the mechanisms of drug disposition and pharmacokinetics (PK) in children following a variety of administration routes. Simulation tools allow exploring the sensitivity of exposure to individual processes involved in drug absorption, distribution, and elimination, and so can help in design of the trials to maximize their efficiency. Several studies were published in the past demonstrating the accuracy of PBPK models in predicting pediatric PK for compounds with simple (perfusion-limited) tissue distribution and elimination mainly by CYP metabolism. For this study, vancomycin (VCN) was selected for its very low membrane permeation that is not captured well by perfusion-limited tissue models, and for its elimination by renal secretion. Rapid changes in glomerular filtration rate (GFR) in the first few weeks after birth and the effect of both gestational age (GA) and postnatal age (PNA) add to the variability in clearance in neonates. Changes in body water content and distribution also affect drug distribution throughout the body and need to be accounted for when trying to predict PK for this age group.

Methods

VCN pharmacokinetics was simulated using the PBPKPlus™ module in GastroPlus™ 9.0 (Simulations Plus, Inc., Lancaster, CA). To account for the low diffusion of VCN through cell membranes, all tissues were treated as permeability-limited tissues. Organ weights, volumes, and blood perfusion rates were generated by the program's internal Population Estimates for Age-Related (PEAR™) Physiology™ module. Renal clearance was estimated from GFR and fraction unbound in plasma (Fup*GFR). Tissue/plasma partition coefficients (Kp's) were calculated using Poulin's equation for drug partitioning into extracellular space (Poulin 2002) from *in vitro* and *in silico* physicochemical properties (ADMET Predictor™ 7.2, Simulations Plus, Lancaster, CA). The permeability-surface area products (PStcs) for individual tissues were calculated as the product of the Specific PStc (PStc per mL of tissue cell volume) and total cell volume of each tissue. The single value of Specific PStc used for all tissues was fitted against *in vivo* plasma concentration-time (Cp-time) data after *i.v* administration of VCN in rats. The model was subsequently used to predict the VCN PK in human adults. After validating against adult data, the model was used to predict VCN PK in different pediatric groups, including neonates and infants. The importance of GA vs PNA on VCN PK was explored.

Conclusions

This study demonstrates the utility of PBPK modeling throughout the drug development continuum, starting with modeling in preclinical species, followed by first-in-human prediction, and finally predicting PK in pediatric groups. PBPK methodology also offers the opportunity to isolate contributions of individual physiological processes, to explore the sources of variability in PK, and to highlight the physiological parameters to consider when deciding the starting dose for individual patients. The presented example also shows the application of predicting pediatric PK for a compound where the distribution is not well-predicted by standard methods for tissue/plasma partition coefficients and requires characterization of the kinetics of diffusion through the cell membranes.

Results

The PBPK model was calibrated by fitting Specific PStc (fitted value 2.5e-5 mL/s/mL cell volume) against the observed Cp-time profile after 5mg/kg i.v. administration of VCN in rats, and verified by predicting VCN plasma and kidney concentrations in rats after 100 mg/kg i.v. administration (Figure 1). The model developed using PK data in rats resulted in excellent prediction of VCN PK in adult humans (Figure 2). Finally, the model was successfully scaled to predict PK in children, including neonates and infants. By accounting for the effects of both GA and PNA on the ontogeny of GFR, and changes in body water, the model using built-in neonatal physiologies was also able to predict the variability in VCN PK in this age group.

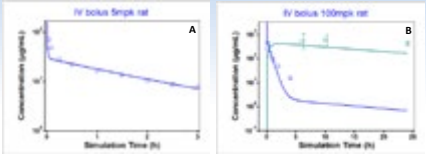

Figure 1: Simulated (lines) and observed (points) VCN plasma (blue) and kidney (dark cyan) concentration time profiles in rat after i.v. administration 5 mg/kg (A) and100 mg/kg dose (B). The Cp-time profile after 5mg/kg dose was used to calibrate the model (fit Specific PStc value). Both plasma and kidney concentration-time profiles after 100 mg/kg dose were predicted using the Specific PStc fitted against only the plasma data for 5 mg/kg dose. Experimental data were obtained from [1-2]. Simulations were performed using default rat physiologies in GastroPlus 9.0, experimental Fup and GFR as reported in each study, and an *in silico* (ADMET Predictor v7.2) value for blood/plasma concentration ratio (Rbp = 0.68)

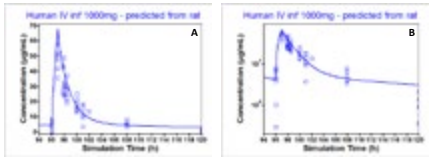

Figure 2: Simulated (lines) and observed (points) VCN steady-state Cp-time profile after i.v. administration of 1000 mg dose in healthy adult volunteers shown on linear scale (A) and log scale (B). Experimental data were obtained from [3]. Simulations were performed using default physiology and GFR in GastroPlus 9.0 for adult human matching age and weight of subjects from the reported study (24-years-old, 84.3kg), experimental Fup [4], *in silico* (ADMET Predictor v7.2) value for Rbp, and Specific PStc as fitted against observed VCN Cp-time profile in rats.

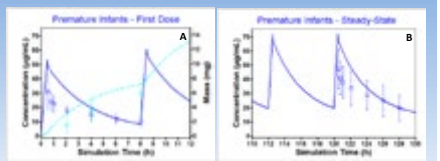

Figure 3: Predicted (lines) and observed (points) VCN Cp-time profile (blue) and cumulative amount excreted in urine (cyan) in premature infant (20-days-old, born 12 weeks premature, body weight 1.07kg) after i.v. administration of 12.6 mg/kg dose after first dose (A) and in steady-state (B). Experimental data were obtained from [5]. Simulations were performed using default physiology and GFR in GastroPlus 9.0 for premature infant matching GA, PNA, and weight of subjects from the reported study. Fup and Rbp scaled from adult values using the built-in scaling function in GastroPlus 9.0 based on age-dependent changes in plasma albumin levels and hematocrit, and Specific PStc calibrated using rat data (Figure 1), and validated by simulation of adult human PK (Figure 2).

Sensitivity analysis was performed to explore the effect of rapid physiological changes in the first few weeks after birth as well as the effect of GA and PNA on the PK of VCN in neonates and infants. Default physiologies for infants with GA 25 to 40 weeks and PNA 2 days to 20 weeks were generated using built-in algorithms in GastroPlus 9.0. VCN PK after 15 mg/kg i.v. dose was simulated for each virtual infant and clearance was calculated from dose and simulated AUC. The simulated CL was compared to the variability in CL from a Population PK (PopPK) model fitted to data from an infant clinical study [6]. The PBPK model resulted in excellent *a priori* prediction of VCN CL in this age group (Figure 4) by considering the influence of both GA and PNA on ontogeny of GFR (Figure 5).

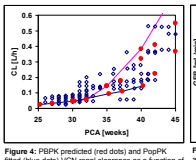

Figure 4: PBPK predicted (red dots) and PopPK fitted (blue dots) VCN renal clearance as a function of post-conceptional age (PCA = GA + PNA). Magenta line shows changes in VCN CL for GA = 30 weeks and varying PNA; blue line shows changes in VCN CL for PNA = 2 days and varying GA as predicted by PBPK model. Simulations were performed using default physiologies and GFR in GastroPlus for infants with varying GA and PNA, Fup and Rbp were scaled from adult values using the built-in scaling function in GastroPlus 9.0 based on age-dependent changes in plasma albumin levels and hematocrit.

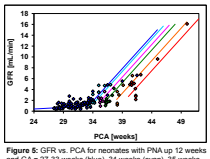

Figure 5: GFR vs. PCA for neonates with PNA up 12 weeks and GA = 27-33 weeks (blue), 34 weeks (cyan), 35 weeks (magenta), 36 weeks (green), 38 weeks (orange) and 40 weeks (red). GFR is increasing very slowly with GA during intrauterine development. For neonates born after at least 34 weeks of gestation, the GFR will start increasing rapidly immediately after birth. For neonates born before 34 weeks of gestation, the slow maturation of GFR from intrauterine development continues until ~34 weeks of PCA before the onset of the fast maturation phase. Lines represent built-in models in GastroPlus 9.0 [7] and points represent experimental data [7 and references therein]

References

[1] Shimada – Anticancer Res 2012, 32: 823-829
[2] Kusama – J Pharm Sci 1998, 87: 1173-1176
[3] Lodise – Antimicrob Agents Chemother 2011, 55: 5507-5511
[4] Butterfield – Antimicrob Agents Chemother 2011, 55: 4277-4282
[5] Reed – Ped Res 1987, 22: 360-363
[6] Grimsley – Arch Dis Child Fetal Neonatal Ed. 1999, 81: F221-F227
[7] GastroPlus manual, version 9.0 (Simulations Plus, Inc.)

T3312

Physiologically Based Pharmacokinetic Modeling of Rosuvastatin and Prediction of Transporter-Mediated Drug-Drug Interactions Involving Gemfibrozil

Joyce S. Macwan[1], Viera Lukacova[1], Grazyna Fraczkiewicz[1], Michael B. Bolger[1], Fatemeh Akhlaghi[2], Walter S. Woltosz[1]

[1]Simulations Plus, Inc., 42505 10th Street West, Lancaster, California 93534, USA . [2]University of Rhode Island, Kingston, Rhode Island 02881, USA

PURPOSE

Rosuvastatin (Crestor®) is a commonly prescribed lipid-lowering agent from the statin drug class for the treatment of primary hyperlipidemia and hypertriglyceridemia. It may be coprescribed with another lipid-lowering drug such as gemfibrozil due to their complementary effect. Rosuvastatin is a substrate of multiple transporters including organic anion transporting polypeptides 1B1 (OATP1B1), 1B3 (OATP1B3), 2B1 (OATP2B1), as well as sodium-taurocholate cotransporting polypeptide (NTCP) and breast cancer resistance protein (BCRP), and exhibits minor metabolic clearance. Gemfibrozil is an inhibitor of the OATP1B1 transporter, which accounts for ~50% of the active liver uptake clearance of rosuvastatin. Studies have reported that concomitant administration of statins and gemfibrozil is associated with an increased risk of myopathy and rare but life-threatening rhabdomyolysis, possibly caused by increased systemic exposure of statins. Patients with genetic polymorphisms may be at a higher risk of severe drug interactions when rosuvastatin and gemfibrozil are coprescribed. The objective of this study was to develop a physiologically based pharmacokinetic (PBPK) model of rosuvastatin following oral administration, and to apply this model to predict the transporter-mediated drug-drug interactions with gemfibrozil.

METHODS

- The GastroPlus™ 9.0 (Simulations Plus, Inc.) Advanced Compartmental Absorption and Transit™ (ACAT™) model was used in conjunction with the PBPKPlus™ and Metabolism and Transporter modules to build a mechanistic absorption/PBPK model for rosuvastatin.
- Physicochemical and biochemical parameters that predict absorption and distribution were obtained from literature [1] or were predicted from structure with ADMET Predictor™ 7.2 (Simulations Plus, Inc.).
- Human organ weights, volumes, and blood perfusion rates were generated by the Population Estimates for Age-Related (PEAR™) Physiology™ module.
- All tissues except the liver were modeled as perfusion-limited tissues. Tissue/plasma partition coefficients (Kps) of perfusion-limited tissues were calculated using the Berezhkovskiy method [2] based on tissue composition and *in vitro* and *in silico* physicochemical properties.
- Intestinal passive absorption, BCRP-mediated active efflux, and enterohepatic circulation of rosuvastatin were incorporated in the PBPK model. The permeability-limited liver model included active sinusoidal uptake, passive diffusion, metabolism, and biliary secretion mediated by active canalicular efflux (**Figure 1**).
- *In vitro* Km values for OATP1B1, OATP1B3, NTCP and BCRP transporters were obtained from literature [3-5]. V_{max} values for the liver uptake transporters were fitted against *in vivo* data to match estimated contribution of each transporter (~50% for OATP1B1, ~35% for NTCP and ~16% for OATP1B3) to the total active hepatic uptake of rosuvastatin [5-6].
- The model was validated by comparing simulated and observed plasma concentration-time profiles for parent drug across several different dose levels following single and multiple oral administrations obtained from literature [7-12].
- Intestinal passive absorption and metabolic clearance both in gut (CYP3A4) as well in permeability-limited liver (CYP3A4 and UGT2B7) were included in gemfibrozil model. MRP transporter-mediated biliary secretion, renal clearance, enterohepatic circulation and parent to metabolite interconversion were incorporated in disposition of gemfibrozil glucuronide metabolite.
- OATP1B1 and NTCP transporter-mediated drug-drug interactions were predicted with the GastroPlus DDI module through dynamic simulations using the validated rosuvastatin and gemfibrozil PBPK models
- IC_{50} for gemfibrozil inhibition of rosuvastatin OATP1B1- and NTCP-mediated liver uptake was from the literature [5,10]

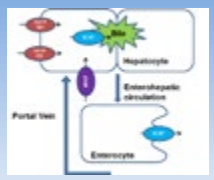

Figure 1. Overview of the major processes governing the disposition of rosuvastatin in gut and liver.

RESULTS

- The model adequately described hepatobiliary disposition and dose proportional pharmacokinetics of rosuvastatin over the dose range of 10 to 80 mg in different populations of subjects following an oral administration (**Figure 2A, B, C and D**)

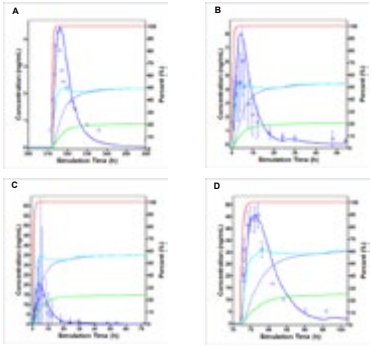

Figure 2. Observed (points) and simulated (lines) plasma concentration-time profiles of rosuvastatin after multiple doses of 10 mg (A), single dose of 20 mg (B), single dose of 40 mg (C), and single dose of 80 mg (D) in healthy volunteers. Experimental data were obtained from literature [7-10]. Amount dissolved (red), amount absorbed (cyan) cumulative amount that entered portal vein (blue) and cumulative amount that entered systemic circulation (green).

- The simulated AUC_{0-t}, C_{max} and t_{max} values were within 1.5-fold of the observed data following (10-80 mg) oral doses of rosuvastatin.
- The predicted increase in plasma AUC_{0-t} and C_{max} of rosuvastatin in the presence of gemfibrozil was approximately 2-fold, which was in close agreement with observed values [5] as shown in **Table 1** and **Figure 3A**.
- The inhibitory effect of gemfibrozil on activity of uptake transporters resulted in identical fold change in AUC_{0-t} and C_{max} of muscle and plasma (**Figure 3B**).

C_{max} Ratio			AUC Ratio		
Observed	Predicted		Observed	Predicted	
Plasma	Plasma	Muscle	Plasma	Plasma	Muscle
2.21	2.13	2.12	1.88	1.95	1.95

Table 1. Summary of observed and predicted DDI of rosuvastatin with gemfibrozil.

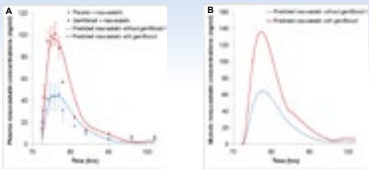

Figure 3. Observed (points) and simulated (lines) plasma (A) and muscle (B) concentration-time profiles of rosuvastatin after an oral dose of 80 mg with oral gemfibrozil pretreatment (600 mg twice daily for 7 days) or placebo. Experimental data were obtained from the literature [10].

CONCLUSIONS

- The absorption and pharmacokinetics of rosuvastatin were accurately modeled using only *in vitro* data. The model successfully predicted the drug-drug interaction related to inhibition of OATP1B1- and NTCP-mediated rosuvastatin hepatic uptake by gemfibrozil.
- Increased muscle levels of rosuvastatin upon concomitant administration of gemfibrozil may explain high risk of muscle-related side effects.
- This model can be extended for quantitative prediction of the impact of genetic polymorphisms and drug-drug interactions mediated by OATP, NTCP, and BCRP inhibitors.
- The model can help to identify populations at increased risk for side effects and to optimize their dosing regimens for the safe and effective use of rosuvastatin.

REFERENCES

1. Jones et al. Drug Metab Dispos. 2012; 40(5):1007-17
2. Berezhkovskiy, J Pharm Sci. 2004; 93(6):1628-40
3. Huang et al. Drug Metab Dispos. 2006; 34(5):738-42
4. Deng et al. Pharm Res. 2008; 25(8):1807-14
5. Ho et al. Gastroenterology. 2006; 130(6):1793-806
6. Kitamura et al. Drug Metab Dispos. 2008; 36(10):2014-23
7. Martin et al. Br J Clin Pharmacol. 2002; 54(6):672-7
8. Martin et al. Clin Ther. 2003; 25(11):2822-35
9. Martin et al. Clin Ther. 2003; 25(10):2553-63
10. Schneck et al. Clin Pharmacol Ther. 2004; 75(5):455-63
11. Martin et al. Clin Ther. 2003; 25(8):2215-24
12. Pasanen et al. Clin Pharmacol Ther. 2007; 82(6):726-33

T8080

Application of Physiologically Based Pharmacokinetic (PBPK) Models in Predicting Drug Pharmacokinetics for Different Ethnic Groups

Ke X. Szeto*, Viera Lukacova*, Min Li +, Haiying Zhou*, John DiBella*, Walter S. Woltosz*, and Michael B. Bolger*

* Simulations Plus, Inc., 42505 10th Street West, Lancaster, CA 93534, USA

+ Department of Biostatistic and Clinical Pharmacology, CFDA, China

CONTACT INFORMATION: KEXU@SIMULATIONS-PLUS.COM

2017 AAPS ANNUAL MEETING & EXPOSITION

DEVELOPING SCIENCE. IMPACTING HEALTH.

PURPOSE

The purpose of this study was to evaluate the ability of PBPK models to predict the pharmacokinetics (PK) of different compounds in two ethnic groups, Caucasian and Chinese. The test set included compounds that have different clearance mechanisms. The population difference was captured by the built-in physiologies provided in GastroPlus™ (Simulations Plus, Inc.), which accounted for the differences in tissue sizes, blood flow rates, enzyme expression levels, glomerular filtration rates, plasma protein binding, and other factors in the two population groups.

METHOD(S)

The PBPKPlus™ module in GastroPlus was used to model the PK for multiple drug compounds, which have different enzymatic clearance (Table 1) and varying fractions of renal secretion. The Advanced Compartmental Absorption and Transit (ACAT™) model was used to describe the intestinal dissolution, precipitation, absorption, and intestinal metabolism (where applicable) after oral (p.o.) administration. The default dissolution model was used for most of the compounds. Human physiologies were generated by the program's internal Population Estimates for Age-Related (PEAR™) Physiology™ module. The Chinese physiology model is based on multiple publications and the weight and height data is based on the China Health and Nutrition survey data (CHNS). The organ sizes are calculated as functions of age, weight and height (and/or other parameters such as bioimpedance, BSA).

Tissue/plasma partition coefficients for most compounds were calculated by the default Lukacova algorithm (some used measured Kp values for a few tissues) based on tissue composition and *in vitro* and *in silico* physicochemical properties. Physicochemical and biopharmaceutical properties for all compounds (and metabolites, where applicable) were either obtained from literature or predicted by ADMET Predictor™ (Simulations Plus, Inc.). Metabolic reactions were modelled by Michaelis-Menten kinetics with built-in expression levels of each particular enzyme in gut and liver for the corresponding populations. Enzyme kinetic parameters (Km and Vmax) were used as reported in literature from *in vitro* experiments or fitted against *in vivo* plasma concentration-time (Cp-time) profiles in Caucasian populations only.

Table 1. Modeling details for the list of compounds

Compound	Theophylline	Ketoconazole	Atomoxetine	Fluconazole
BCS Class	I	II	I	I
Main Clearance Pathway	CYP 1A2	CYP 3A4	CYP 2D6 CYP 2C19	Renal
Num of Data Sets	8	7	7	10
Dosage Forms	IV, Tab	Tab	Cap	IV, Cap, Tab
Compound	**Gemfibrozil**	**Midazolam**	**Rifampicin**	**Tolbutamide**
BCS Class	II	I	II	II
Main Clearance Pathway	CYP 3A4 UGT 2B7	CYP 3A4	Esterase, CYP 3A4, Renal	CYP 2C9
Num of Data Sets	9	10	5	7
Dosage Forms	Tab, Cap	IV, Tab, Sol	Cap, Tab	IV, Tab

RESULT(S)

The model accurately described the mean Cp-time profiles for the listed compounds and their metabolites (where applicable) for different doses and formulations in both populations and explained inter-ethnic differences in the PK of specific compounds. The detailed information of each compound is given in Table 1. The overall prediction errors for Cmax and AUC averaged across all compounds/studies are both less than 20%: 15.9% for Cmax and 17.1% for AUC. Some compounds exhibit more pronounced population differences, such as midazolam (AUC difference > 70%), and some compounds have only minimal effects, such as rifampicin (AUC difference < 20%). Predictions of representative studies for 5 of the 8 test compounds are shown in Figures 1-5, where we presented those with most distinct clearance pathways. Studies with similar dose amounts and formulations in Chinese and Caucasian subjects were selected to show for an easy comparison of inter-ethnic differences.

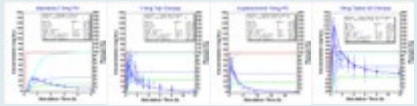

Figure 1: Simulated and observed midazolam Cp-time profiles after administration of midazolam tablet in fasted Caucasian and Chinese adults. A. 7.5 mg midazolam in a 22-year-old, 69 kg Caucasian male. **B.** 7.5 mg midazolam in a 23-year-old, 63.6 kg Chinese male. **C.** 15 mg midazolam in a 25-year-old, 70 kg Caucasian male **D.** 15 mg midazolam in a 40-year-old, 67.3 kg Chinese male. Km and Vmax values for 3A4 were from [Paine 1997].

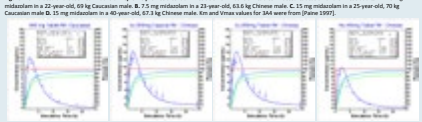

Figure 2: Simulated and observed rifampicin Cp-time profiles after rifampicin administration in fasted Caucasian and Chinese adults. A. 600 mg rifampicin tablet in a 30-year-old, 70kg Caucasian male. **B.** 600 mg rifampicin capsule in a 21-year-old, 62.8 kg Chinese male. **C.** 600 mg rifampicin tablet in a 21-year-old, 62.8 kg Chinese male. **D.** 450 mg rifampicin tablet in a 22-year-old, 65.5 kg Chinese male. Esterase and renal clearance were derived from [Lau 2007]. Km for 3A4 was from [Kajosaari 2005] and Vmax value was estimated from [Lau 2007].

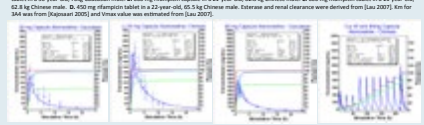

Figure 3: Simulated and observed atomoxetine Cp-time profiles after administration of atomoxetine capsule in fasted Caucasian and Chinese adults. A. 20 mg atomoxetine in a 52-year-old, 81 kg Caucasian male. **B.** 20 mg atomoxetine in a 24-year-old, 59 kg Chinese male. **C.** 90 mg atomoxetine in a 30-year-old, 74 kg Caucasian male. **D.** 40 and 80 mg atomoxetine (40 mg once daily (qd) for 3 days (days 1, 2 and 3), followed by atomoxetine 80 mg qd for 7 days (days 4–10)) in a 30-year-old, 62 kg Chinese male of 62 kg. Km values were from [Ring 2002] and Vmax values were fitted.

NOTE: in all plots, the dark blue colored lines and data points represent plasma concentrations (shown on the left Y-axis). The red, cyan, light blue and green colored lines are cumulative percents of the dose dissolved, absorbed, entering portal vein and entering systemic circulation, respectively (shown on the right Y-axis). The observed data are from multiple publications listed in the references and the subject weight and age are averages of the subjects in these studies.

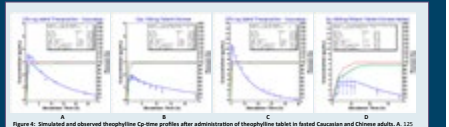

Figure 4: Simulated and observed theophylline Cp-time profiles after administration of theophylline tablet in fasted Caucasian and Chinese adults. A. 125 mg theophylline in a 30-year-old, 62 kg Caucasian male. **B.** 100 mg theophylline in a 30-year-old, 69 kg Chinese male. **C.** 375 mg theophylline in a 30-year-old, 62 kg Caucasian male. **D.** 350 mg theophylline (as modified release tablet) in a 25-year-old, 63 kg Chinese male. The controlled released profile used in the GastroPlus simulation was from published in vitro dissolution data. Km for 1A2 was from [Tjia, 1996] and Vmax value was fitted.

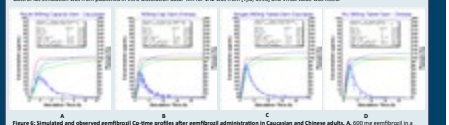

Figure 6: Simulated and observed gemfibrozil Cp-time profiles after gemfibrozil administration in Caucasian and Chinese adults. A. 600 mg gemfibrozil in a 30-year-old, 70 kg Caucasian male. **B.** 600 mg gemfibrozil in a 21-year-old, 59.8 kg Chinese male. **C.** 900 mg gemfibrozil in a 30-year-old, 65 kg Caucasian male. **D.** 900mg gemfibrozil in a 25-year-old, 65.5 kg Chinese male. The percent entered portal vein is over 100%, which is caused by the conversion of the glucuronide metabolite back to the parent compound in the intestine. Km for UGT2B7 was from [Mano 2007] and Vmax value was fitted.

CONCLUSION(S)

The work described the use the mechanistic absorption model/ physiologically based pharmacokinetic MAM/PBPK approach for drug development and demonstrates the ability to predict inter-ethnic differences in PK over a range of compounds. The current approach helps to quantify dose regimens for different ethnic groups; hence, it will be very useful in a number of areas including drug safety, pharmacodynamics, and drug-drug interactions. The MAM/PBPK approach incorporates all of the relevant processes in drug absorption, distribution, metabolism, and elimination, and facilitates prediction of PK for different dosage forms and study designs.

REFERENCES

[1]CHNS China Health and Nutrition Survey. http://www. cpc.unc.edu/projects/china. Accessed Jan 5th 2016
[2] Wang, Chinese Journal of Radiological Medicine and Protection 15(4), 1995
[3]. Li, Chin J Pathol 25(2), 1996
[4] Reference individuals for use in radiation protect – Part 3: main physiological parameters, GB2/T 200.3, 2014
[5] Li, Journal of Guangxi Medical University 23(1), 2006
[6]Wang et al, Acta Academiae Medicinae Jiangxi 29(5), 1989
[8] Wang Journal of Enshi Medical Institute 7(2), 1990
[9] Yang, Acta Pharmaceutica Sinica 50(6), 2015
[10] Shu, Acta Pharmacol Sin 22(3), 2001
*note, this is only a selected list

SimulationsPlus SCIENCE + SOFTWARE = SUCCESS

T4056

Development of *In Vitro-In Vivo* Correlation for Long Acting Injectable Microsphere Formulations

A. Shahraz, J. Mullin, J. Spires, V. Lukacova, M. B. Bolger, W. Woltosz
Author Affiliation: Simulations Plus, Inc

CONTACT INFORMATION: azar@simulations-plus.com

2017 AAPS ANNUAL MEETING & EXPOSITION

DEVELOPING SCIENCE. IMPACTING HEALTH.

PURPOSE

The concept of *in vitro-in vivo* correlations (IVIVCs) for long-acting injectable (LAI) microsphere formulations has gained more significance in the past decade. However, this problem is challenging due to the multiphase release characteristics of compositionally equivalent formulations, the lack of a mechanistic deconvolution method, and the lack of compendial *in vitro* release testing methods. This study aims to (1) determine whether an IVIVC can be established for long-acting injectable microsphere formulations with different release profiles; (2) assess the role of mechanistic deconvolutions in determining the *in vivo* release profiles; and (3) explore the potential for using a triphasic Weibull function on improving results of the deconvolution process.

OBJECTIVE(S)

The Objectives of this study are to investigate the feasibility of establishing IVIVC for long acting injectable microsphere formulations and to discover important aspects of this process.

METHOD(S)

We attempted to establish validated Level A IVIVCs using GastroPlus™ 9.6 (Simulations Plus, Inc.) for several drugs formulated as long-acting injectable microspheres. Literature data for several poly (d,l- lactide-co-glycolide) (PLGA) or poly(d,l-lactide) (PLA) formulations administered subcutaneously in Sprague-Dawley rats for olanzapine [1], intramuscularly in beagle dogs for huperzine A [2], and subcutaneously in rats for orntide [3] were used in this study. For each case study, the PK was established based on plasma concentration-time (Cp-time) profiles after intravenous (IV) (huperzine A), intraperitoneal (IP) (olanzapine), or subcutaneous (SC) (orntide) injection. The PK model was subsequently linked to the intramuscular or subcutaneous controlled release model in the Additional Dosage Routes Module (ADRM) in GastroPlus, and the complete model was used to deconvolute the *in vivo* release profile for each formulation. Finally, level A IVIVCs between the deconvoluted *in vivo* release and *in vitro* dissolution profiles were established and evaluated across different formulations for each test compound.

RESULT(S)

A level A IVIVC was established for each of the test compounds and formulations and several important aspects were discovered in the process.

(1) Complex *in vivo* Profile: The *in vivo* release profiles for these long-acting injectable microspheres may be complex and cannot be always accurately described by a single- or double-Weibull function. A triple-Weibull function was required to accurately describe the *in vivo* release profiles for orntide formulations.

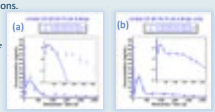

*Simulated Cp-time profiles after SC injection of one orntide LAI formulation in rat. The in vivo release profile was fitted as **(a)** double-Weibull and **(b)** triple-Weibull function.*

(2) Optimization Target Criteria: When fitting the *in vivo* release profile against the entire observed Cp-time profile, the error on Cmax is often higher than allowed by the IVIVC criteria due to the number of other concentration points outweighing the contribution of the single Cmax value. This issue can be addressed by including additional weight on Cmax during the deconvolution/optimization process.

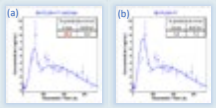

*Simulated Cp-time profiles for a naltrexone LAI microsphere formulation considering **(a)** target observed Cp-time profile and **(b)** additional weight added to Cmax in the optimization function.*

(3) Insufficient *in vitro* Sampling: The density of *in vitro* sampling points is also important for prediction of the correct shape of the Cp-time profile. In the case of huperzine A, the IVIVC was able to predict the Cmax and AUC for new formulations, but a smaller initial peak was not captured due to the lack of *in vitro* data points representing the initial release of the drug. This limitation was addressed by using interpolated data points in the *in vitro* dissolution profile.

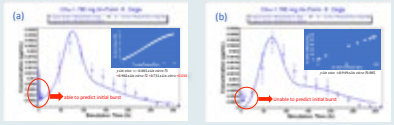

*Predicted Cp-time profiles for a huperzine A LAI microsphere formulation based on IVIVC built **(a)** with and **(b)** without using the interpolated in vitro data*

CONCLUSION(S)

The possibility of establishing IVIVCs for long-acting injectable microsphere formulations was investigated. The results show promise, but the desired success is yet to be achieved. Several important aspects have been discovered, including:

- The significance of using a triple-Weibull function in the mechanistic deconvolution and describing the more complex *in vivo* release of some long-acting injectable microspheres
- The role of the selected optimization objective function in the mechanistic deconvolution, specifically in the case of lacking sufficient *in vivo* sampling points
- The effect of using interpolated *in vitro* data in establishing an IVIVC and predicting the correct shape of the Cp-time profile

We aim to continue our study on the pharmacokinetics of LAI microspheres with the goal of better characterizing the *in vivo* environmental parameters that affect polymer degradation, microsphere dispersion, and API pharmacokinetics after *in vivo* injection of these formulations.

FUNDING / GRANTS / ENCORE / REFERENCE OR OTHER USE

The work was done under funding from the FDA (grant 1U01FD005463-02)

References

[1] D'Souza, S., Faraj, J. A., Giovagnoli, S., DeLuca, P. P., International Journal of Biomaterials 2014; 2014 Article ID 407065
[2] Chu, D., Fub, X., Liu, W. Liu, K., Li, Y., , International Journal of Pharmaceutics 2006; 325: 116–123
[3] Kostanski, J. W., Dani B. A., Reynolds, G., Bowers, C. Y., DeLuca, P. P., , AAPS PharmSciTech 2000; 1 (4).

SimulationsPlus SCIENCE + SOFTWARE = SUCCESS

2980

Application of PBPK Modeling to Predict Monoclonal Antibody Disposition after Intravenous and Subcutaneous Administration in Rats and Humans

Haiying Zhou, Michael B. Bolger, Viera Lukacova
Simulations Plus, Inc., 42505 10th Street West, Lancaster, CA 93534, USA

PURPOSE

Therapeutic monoclonal antibodies (mAbs) represent a growing segment of the development pipeline in the pharmaceutical industry. Physiologically based pharmacokinetic (PBPK) modeling has been extensively applied in small molecule drug development and has a great potential of helping in the development of mAbs and functional derivatives. In this study, a comprehensive PBPK model for mAbs was developed to simulate plasma as well as individual tissue concentrations after intravenous (IV) or subcutaneous (SC) administration in preclinical animals and humans.

METHODS

The whole-body PBPK model previously developed in GastroPlus™ (Simulations Plus, Inc.) was expanded to include mechanisms related to the absorption and disposition of mAbs. Each organ in the PBPK model is divided into three major compartments representing the vascular, endosomal, and interstitial spaces, as shown in Figure 1.

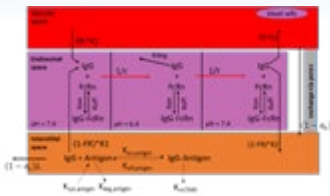

Figure 1: Schematic representation of individual tissue compartments

The following mechanisms are included in the PBPK model:

- Transport of mAb into the tissue interstitial space via convective flow through the paracellular pores in the vascular endothelium
- Uptake of mAb from the vascular and interstitial spaces into the endosomal space via fluid-phase endocytosis
- pH-dependent binding of mAb to FcRn in the endosomal space
- FcRn binding competition between therapeutic mAb and endogenous IgG
- Recycling of mAb to the vascular and interstitial spaces
- Endosomal degradation of the unbound mAb
- Return of mAb from the tissue to the bloodstream through convective transport with lymph flow
- Specific mAb binding to antigen (TMDD)

After SC injection, the mAb was initially distributed in the interstitial space of the local subcutaneous tissue. The local tissue was also divided into three compartments as shown in Figure 1. The same endosomal nonspecific clearance processes were applied to both the systemic clearance and local first-pass clearance after SC administration.

Convective transport through the lymphatic endothelium and fluid-phase endocytosis are the main mechanisms of absorption into the systemic circulation following SC administration of mAb.

The vascular (σ_v) and lymph (σ_L) reflection coefficients, and the fraction of mAb recycled (FR) were obtained from literature (Garg & Balthasar, J Pharmacokinet Pharmacodyn, 34 (2007), 687-709). Other model parameters (pH-dependent mAb-FcRn binding constants, mAb degradation in endosomal space, endosomal uptake, and recycle rates) were fitted using datasets from studies of 14 different antibodies and the reported synthesis rate of endogenous IgG (Junghans, Blood, 90 (1997), 3815-3818; Cure & Cremer, J Immunol, 102 (1969), 1345-1353) for different species. The fitted mAb-FcRn binding constants were within the range of reported *in vitro* values (Datta-Mannan et al., J Biol Chem, 282 (2007), 1709-1717; Andersen et al., J Biol Chem, 285 (2010) 4826-4836).

RESULTS

The PBPK model for mAbs was used to simulate plasma concentration-time profiles of MEDI-528 in human and Rituximab in rats across different dose levels after IV and SC administration. The simulated profiles were in close agreement with published clinical results (White et al., Clin Ther, 31 (2009), 728-740; Kagan et al., Pharm Res, 29 (2012), 490-499).

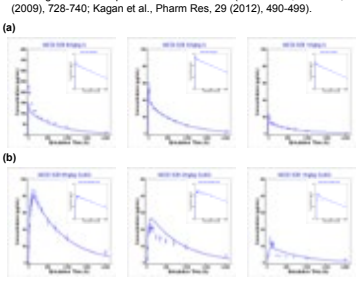

Figure 2: Comparison of simulated (lines) and measured (points) MEDI-528 for 9, 3, and 1 mg/kg doses in healthy subjects after IV **(a)** and SC **(b)** doses.

Default model parameters for human were used for MEDI-528 simulations.

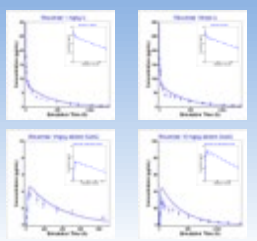

Figure 3: Comparison of simulated (lines) and measured (points) for Rituximab for 1 and 10 mg/kg doses in Wistar rats after IV **(a)** and SC **(b)** doses

The association coefficient between Rituximab and rat FcRn was estimated using the data from the 1 mg/kg IV dose. For the simulation of Rituximab in rats after SC administration, an additional linear clearance was included in the local first-pass clearance in addition to the endosomal nonspecific clearance processes and was estimated using the data from the 1 mg/kg SC dose. Other parameters used the default GastroPlus values for rat.

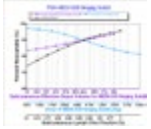

SC bioavailability is sensitive to dose, subcutaneous lymph flow, and effective depot volume:

- Bioavailability decreases as dose increases
- Bioavailability increases as the lymph flow or effective depot volume increases

Figure 4: Parameter sensitivity of bioavailability

CONCLUSIONS

- PBPK modeling of mAbs in GastroPlus accurately simulates PK profiles after IV and SC administration.
- This model can help to investigate the factors responsible for the systemic disposition of mAbs in preclinical animals and human.
- This model could also be applied to assess dose-dependent nonlinear clearance related to TMDD

SimulationsPlus SCIENCE + SOFTWARE = SUCCESS

Revised 3/9/18